

**HERG channel (dys)function
revealed by “dynamic action potential clamp” technique**

Supplement

MS BIOPHYSJ/2004/047290

Géza Berecki,^{* #} Jan G. Zegers,[#] Arie O. Verkerk,^{* #} Zahurul A. Bhuiyan,[§] Berend de Jonge,^{*}
Marieke W. Veldkamp,^{*} Ronald Wilders,[#] Antoni C.G. van Ginneken^{*}

From the ^{*}Experimental and Molecular Cardiology Group and the Departments of [#]Physiology
and [§]Clinical Genetics, Academic Medical Center, University of Amsterdam, The Netherlands.

Correspondence to G. Berecki, Department of Clinical and Experimental Cardiology,

Academic Medical Center, University of Amsterdam, Room M01-217;

Street Address: Meibergdreef 9, 1105 AZ Amsterdam, The Netherlands;

Postal Address: PO Box 22700, 1100 DE Amsterdam, The Netherlands;

Phone: +31-20-5667547; *Fax:* +31-20-6919319; *E-mail:* g.berecki@amc.uva.nl

Expanded Materials and Methods

Plasmid construction

The wild-type (WT) human ether-a-go-go-related gene (HERG) cDNA ([Hoppe et al., 2001](#)), cloned in the GFPires plasmid ([Johns et al., 1997](#)) for bicistronic expression of the HERG channel and green fluorescent protein reporter, was kindly provided by Dr. David C. Johns (Johns Hopkins University, Baltimore, MD, USA). WT HERG-GFPires was digested with *SacI* and *XhoI* and the resulting HERG cDNA insert was ligated into CFPires (plasmid with cyano-fluorescent protein reporter), resulting in WT HERG-CFPires. The R56Q (arginine to glutamine) HERG cDNA was made by PCR using the 5'-GCTACTCGCAGGCCGAGGTGATG-3' ("forward") and 5'-CATCACCTCGGCCTGCGAGTAGC-3' ("reverse") primers for overlap-extension mutagenesis. The final PCR product was digested with *SacI* and *XhoI* and ligated into GFPires plasmid, generating R56Q HERG-GFPires. The mutated insert and ligation regions were verified by automated sequencing.

HEK-293 cell transfection and electrophysiological experiments

HEK-293 cells were transiently transfected with WT and/or mutant (R56Q) HERG cDNA using lipofectamine (Invitrogen) and cultured at 37°C. HERG currents (I_{HERG}) were recorded within 1 to 2 days from HEK-293 cells exhibiting cyano and/or green fluorescence, in the whole-cell configuration of the patch-clamp technique, at $23 \pm 0.5^\circ\text{C}$ and $36 \pm 0.5^\circ\text{C}$. The current-voltage (I-V) relationships, activation, deactivation, and inactivation kinetics of the I_{HERG} were determined by voltage clamp protocols as diagrammed in Figs. 2 and 3 of the manuscript and described previously ([Sanguinetti et al., 1995](#); [Smith et al., 1996](#); [Snyders and Chaudhary, 1996](#)). For all

protocols, we used holding potentials of -80 mV and 15-s pacing intervals. To construct the activation curves, tail current amplitude during P2 (see protocol in Fig. 2 *A* in the main manuscript) was normalized to the maximum tail current amplitude and plotted against voltage of P1. The inactivation curves (see protocol in Fig. 2 *B*) were obtained using peak of the tail currents measured during P3 and plotted against voltage of P2. These curves were fitted by the Boltzmann equation $I/I_{\max}=1/\{1+\exp[(V_{1/2}-V)/k]\}$ to determine the membrane potential for half-maximal (in)activation $V_{1/2}$ and the slope factor k . Time constants of activation (see protocol in Fig. 2 *A*) were obtained by fitting the onset of currents during P1 by a mono-exponential equation $I/I_{\max}=A[1-\exp(-t/\tau)]$ (Sanguinetti et al., 1995; Snyders and Chaudhary, 1996; Zhou et al., 1998), where A is amplitude, t is time, and τ is time constant. To obtain the time constants of deactivation, the decaying phase of the current during P2 (see protocol in Fig. 2 *C*) was fitted by the bi-exponential equation $I/I_{\max}=A_f \times \exp(-t/\tau_f) + A_s \times \exp(-t/\tau_s)$, where A_f and A_s are fractions of fast and slow deactivation components, and τ_f and τ_s are the time constants of fast and slow deactivating components, respectively (Sanguinetti et al., 1995). Inactivation was measured using a three-pulse protocol (Fig. 3 *B*, right inset). The first two steps served to (in)activate and recover from inactivation, respectively. The time constants of inactivation were obtained by fitting the declining phase of the current during P3 by the mono-exponential equation $I/I_{\max}=A \times \exp(-t/\tau)$ (Sanguinetti et al., 1995; Snyders and Chaudhary, 1996). Time constants of recovery from inactivation were determined using a two-pulse protocol (Fig. 3 *B*, left inset). P1 served to activate and inactivate HERG channels. Repolarization during P2 elicited a tail current due to fast recovery from inactivation. This recovery process was measured as the fast time constant of a bi-exponential fit to the tail current (the slower time constant of this fit reflects the concurrent deactivation process) (Sanguinetti et al., 1995; Snyders and Chaudhary, 1996; Zhou

et al., 1998). The I-V relationships (see protocol in Fig. 2 C) were determined from the peak of the deactivating tail currents, normalized to the maximum tail current amplitude during P2. P1 activated steady-state I_{HERG} . P2 served to elicit I_{HERG} tails.

Action potential recordings from rabbit myocytes

The Committee for Animal Experiments of the Academic Medical Center approved the experimental protocol. Ventricular myocytes of four New Zealand-White rabbit hearts were isolated according to (Tytgat, 1994). Single cells were stored in Tyrode's solution containing (mmol/L): 140 NaCl, 5.4 KCl, 1.8 CaCl₂, 1 MgCl₂, 5.5 glucose, 5 HEPES (pH 7.4 with NaOH), at room temperature, and were used within 4 h. Myocytes were superfused with Tyrode's solution at 36°C. Action potentials (APs) were measured with the whole-cell configuration of the patch-clamp technique at 36°C, as described previously (Verkerk et al., 1996). The composition of the intracellular solution was identical to that used for HEK-293 cells, except that EGTA was omitted, containing (mmol/L): 125 K-gluconate, 20 KCl, 1 MgCl₂, 5 MgATP, 10 HEPES (pH 7.2 with KOH). Potentials were corrected for liquid junction potential. APs were elicited by 2-ms current pulses ($1.5 \times$ threshold) at 0.2, 1, 2, 3, 4 and 5 Hz. Recordings were low-pass filtered (1-kHz), digitized at 2-kHz and stored on the hard disk of a personal computer. E-4031 (Eisai Pharmaceutical Co.) was dissolved in distilled water as stock solution and used in a final concentration of 5 $\mu\text{mol/L}$. AP parameters, i.e., overshoot, maximum diastolic potential (MDP), action potential amplitude (APA), maximum upstroke velocity (V_{max}), and action potential duration at 50, 80, and 90% repolarization (APD₅₀, APD₈₀, and APD₉₀, respectively), were determined as described previously (Verheijck et al., 1998).

Principles and considerations for scaling WT and R56Q I_{HERG} .

In the PB model (Priebe and Beuckelmann, 1998), the rapidly activating component of the delayed rectifier current (I_{Kr}) is based on experiments on human ventricular myocytes (Li et al., 1996). Other experiments from the literature (Iost et al., 1998) also indicate that I_{Kr} density is correctly estimated in the PB model (see Table 3 in the main manuscript).

Scaling both WT and R56Q I_{HERG} amplitudes to a value equivalent to the original I_{Kr} amplitude in the PB model (47.6 pA) was based on the following observations:

- (i) The transiently expressed WT and R56Q I_{HERG} densities in the HEK-293 cells are statistically not different (see Results).
- (ii) The shape (and amplitude) of the model cell I_{Kr} could genuinely be reproduced with our scaling method (see Fig. 4B, where WT I_{HERG} is a substitute for I_{Kr}).
- (iii) The frequency-dependent behavior of the sustained I_{HERG} component was comparable with WT and R56Q HERG channels (Figs 8 C, D and 9 D).
- (iv) Time constants of inactivation and recovery from inactivation of WT and R56Q HERG channels were similar (Fig 3 B).

The scaling factor (F_s) must vary between cells. This is unavoidable, since expression levels of HERG channels in the HEK-293 cells are also variable.

Scaling WT and R56Q I_{HERG} by normalization to the peak seems to be appropriate here. However, with other mutants, the scaling method should only be decided after having proper insight into fundamental electrophysiological characteristics of the expressed current.

Additional Figures and supporting information

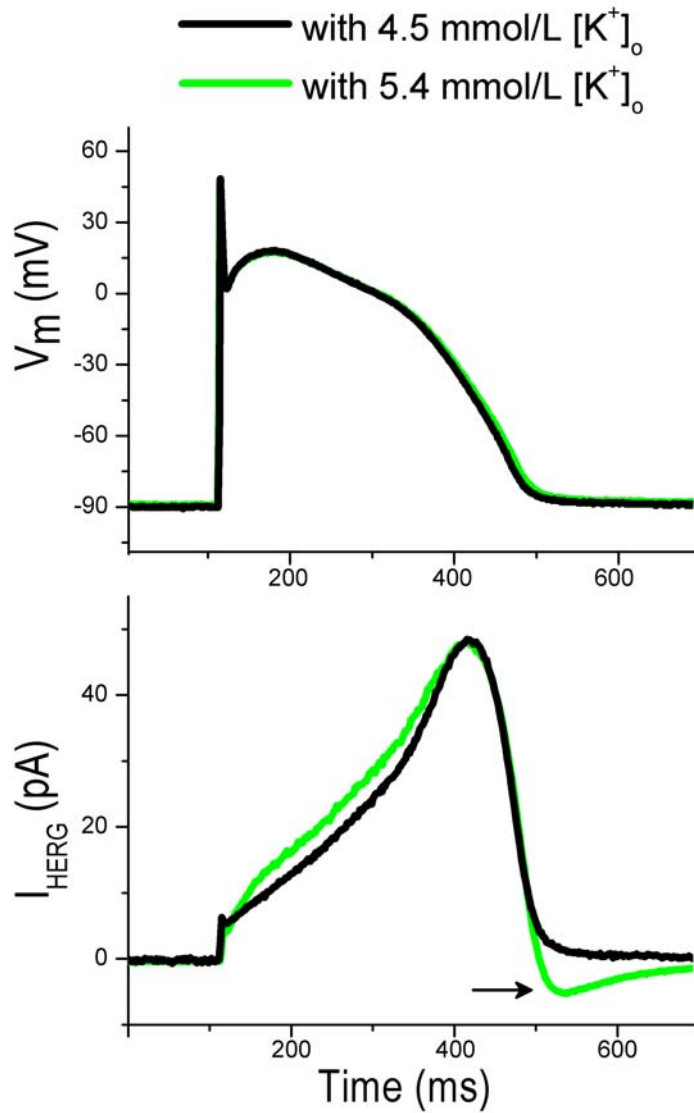


Fig. 1 Time course of the AP waveform-elicited WT I_{HERG} (bottom traces), with 5.4 or 4.5 mmol/L KCl in the Tyrode solution, during dynamic action potential clamp (dAPC) experiments. The maximum diastolic potential (MDP) of the Priebe and Beuckelmann epicardial model cell (Priebe and Beuckelmann, 1998) was -90.7 mV. When the K^+ equilibrium potential (E_K) of the experimental solutions was set to -87.7 mV (with 5.4 mmol/L KCl), an inward I_{HERG} tail current resulted (*arrow*). However, AP characteristics (top traces) were similar in both cases.

Additional Tables and supporting information

Table 1. Time constants of WT and R56Q I_{HERG} activation and deactivation.

I_{HERG}	Recording temperature	τ activation (ms)			τ fast deactivation (ms)			τ slow deactivation (ms)		
		+40 mV	+10 mV	-20 mV	-40 mV	-60 mV	-80 mV	-40 mV	-60 mV	-80 mV
WT	23°C	220	1440	2870	256	196	122	2090	1370	614
	36°C	n.d.	80	470	239	140	51	1550	940	272
R56Q	23°C	270	1100	2580	150*	79*	39*	995*	470*	230*
	36°C	n.d.	31*	210*	84*	32*	12*	497*	110*	21*

Mean values are shown; n.d., not determined; * $P < 0.05$ for R56Q versus WT. See text and Fig. 3 for details.

Table 2. Time constants of WT and R56Q I_{HERG} inactivation and recovery from inactivation.

I_{HERG}	Recording temperature	τ inactivation (ms)			τ recovery from inactivation (ms)		
		+40 mV	+10 mV	-20 mV	-40 mV	-60 mV	-80 mV
WT	23°C	3.7	7.9	11.9	12.3	10.7	7.6
	36°C	1.0	1.8	2.4	2.3	1.8	1.3
R56Q	23°C	3.8	7.9	12.1	11.6	8.8	6.0
	36°C	1.0	1.9	2.5	2.0	1.7	1.4

Mean values are shown. See text and Fig. 3 for details.

Table 3. Action potential parameters of the human ventricular “subepicardial” model cell with I_{Kr} , WT I_{HERG} , and R56Q.

	1 Hz			2 Hz		
	I_{Kr} (n=5)	WT I_{HERG} (n=9)	R56Q I_{HERG} (n=12)	I_{Kr} (n=5)	WT I_{HERG} (n=7)	R56Q I_{HERG} (n=9)
Overshoot (mV)	60.1	55.5±2.2	55.7±1.2	60.1	56.9±2.3	58.6±0.9
MDP (mV)	-90.7	-90.3±0.3	-90.3±0.5	-89.3	-88.1±0.3	-88.6±0.3
APA (mV)	150.7	145.8±1.1	146.0±0.6	149.4	144.0±0.4	147.2±0.5
V_{max} (V/s)	297.8	295.6±3.0	299.6±7.0	291.7	294.6±2.5	300.3±4.6
APD ₅₀ (ms)	242.2	237.4±7.5	268.1±6.1*	228.6	222.4±6.3	249.4±4.3*
APD ₈₀ (ms)	332.5	334.1±7.7	394.3±6.9*	313.2	316.9±5.5	358.8±4.8*
APD ₉₀ (ms)	355.5	359.8±8.3	405.9±7.5*	334.6	346.9±5.9	387.6±4.8*

*P<0.05 for R56Q versus WT. Values are mean±SEM. Results obtained with 5.4 mmol/L KCl in the Tyrode solution.

Table 4. Frequency dependence of action potential duration (APD) in rabbit left ventricular cells.

Frequency (Hz)	Control (n=10)			with WT I _{HERG} (n=5)			with R56Q I _{HERG} (n=5)		
	APD ₅₀	APD ₈₀	APD ₉₀	APD ₅₀	APD ₈₀	APD ₉₀	APD ₅₀	APD ₈₀	APD ₉₀
0.2	168.3±6.8	206.8±10.7	213.2±11.2	175.9±7.2	209.1±10.9	215.1±11.8	209.6±18.3	254.9±14.7*	261.5±13.5*
1	187.6±5.7	224.3±4.5	230.8±4.5	187.9±17.7	227.9±14.2	235.2±7.3	250.7±31.2	309.5±22.7*	317.8±21.9*
2	178.2±4.6	213.5±3.6	219.8±3.6	119.2±35.9	199.6±4.9	207±5.8	177.4±25.0	241.6±19.2	249.8±18.9
3	152.6±3.2	185.8±3.0	192.1±3.2	137.1±1.2	169.1±5.1	173.3±5.2	150.3±10.5	188.7±5.9	194.2±6.4
4	131.9±2.5	163.3±3.0	169.5±3.3	114.4±2.4	149.8±5.5	156.5±6.7	127.2±12.9	168.7±10.9	176.3±11.3

APD₅₀, APD₈₀, and APD₉₀, APD at 50, 80, and 90% repolarization, respectively (mean ± SEM;

*P<0.05 for R56Q versus WT). Control groups represent APDs in the absence of E-4031 (with native I_{Kr} present), while in dAPC experiments (coupling HEK-293 cells expressing WT I_{HERG} or R56Q I_{HERG} to the same rabbit ventricular cell) 5 μmol/L E-4031 was used to block I_{Kr}.

References

- Hoppe, U.C., E. Marbán, and D.C. Johns. 2001. Distinct gene-specific mechanisms of arrhythmia revealed by cardiac gene transfer of two long QT disease genes, HERG and KCNE1. *Proc. Natl. Acad. Sci. U S A.* 98:5335-5340.
- Johns, D.C., H.B. Nuss, and E. Marbán. 1997. Suppression of neuronal and cardiac transient outward currents by viral gene transfer of dominant-negative Kv4.2 constructs. *J. Biol. Chem.* 272:31598-31603.
- Priebe, L. and D.J. Beuckelmann. 1998. Simulation study of cellular electric properties in heart failure. *Circ. Res.* 82:1206-1223.
- Sanguinetti, M.C., C. Jiang, M.E. Curran, and M.T. Keating. 1995. A mechanistic link between an inherited and an acquired cardiac arrhythmia: HERG encodes the I_{Kr} potassium channel. *Cell.* 81:299-307.
- Smith, P.L., T. Baukrowitz, and G. Yellen. 1996. The inward rectification mechanism of the HERG cardiac potassium channel. *Nature.* 379:833-836.
- Snyders, D.J. and A. Chaudhary. 1996. High affinity open channel block by dofetilide of HERG expressed in a human cell line. *Mol. Pharmacol.* 49:949-955.
- Tytgat, J. 1994. How to isolate cardiac myocytes. *Cardiovasc. Res.* 28:280-283.
- Verheijck, E.E., R. Wilders, R.W. Joyner, D.A. Golod, R. Kumar, H.J. Jongasma, L.N. Bouman, and A.C. van Ginneken. 1998. Pacemaker synchronization of electrically coupled rabbit

sinoatrial node cells. *J. Gen. Physiol.* 111:95-112.

Verkerk, A.O., M.W. Veldkamp, A.C. van Ginneken, and L.N. Bouman. 1996. Biphasic response of action potential duration to metabolic inhibition in rabbit and human ventricular myocytes: role of transient outward current and ATP-regulated potassium current. *J. Mol. Cell. Cardiol.* 28:2443-2456.

Zhou, Z., Q. Gong, B. Ye, Z. Fan, J.C. Makielski, G.A. Robertson, and C.T. January. 1998. Properties of HERG channels stably expressed in HEK 293 cells studied at physiological temperature. *Biophys. J.* 74:230-241.